

Adsorption of ferric ion onto defatted seeds of cypress tree: Equilibrium and kinetic studies

Mohammed A. Al-Anber^{1,*}, Zaid Al-Anber², Idrees Al-Momani³¹Department of Environmental Health, Faculty of Public Health and Health Informatics, University of Hail, Hail, King Saudi Arabia²Department of Chemical Engineering, Faculty of Engineering Technology, Al-Balqa University, Amman, P.O Box 15008, Amman 11131, Jordan³Department of Chemistry, Faculty of Science, Yarmouk University, Irbid, Jordan*corresponding author e-mail address: m.alanber@uoh.edu.sa

ABSTRACT

Adsorption of ferric ion onto residues of cypress tree seeds (Defatted Seeds of Cypress Tree; DSCT) has been studied using batch system. Batch experiments have been carried out as a function of initial concentration of ferric ion (Fe^{3+}), the dosage of DSCT, temperature, and agitation period. The equilibrium isotherms system is analyzed by Langmuir and Freundlich adsorption models. The maximum percentage removal achieved is 73 % through the experiments conditions of 5 minutes of adsorption, $T = 50\text{ }^\circ\text{C}$, $C_i = 100\text{ mg L}^{-1}$, $\text{pH} = 1.15$, and dosage = 10 g L^{-1} . Depending on the adsorption thermodynamic model, the adsorption mechanism of aqueous ferric ion onto DSCT follows Freundlich isotherm model ($R^2 = 0.995$). The capacity (K_f) and intensity (n) of Freundlich adsorption are 1.795 and 1.488, respectively. The experimental data are fitted into Lagergren pseudo-first order and pseudo-second order for the kinetic studies. The kinetic parameters, rate constant, equilibrium sorption capacities and related correlation coefficients are calculated for each kinetic model. The pseudo-second order kinetic model has much more reasonable to correlate the experimental data of the sorption system ($R^2 = 1.0$ approx.). Several diffusion models are used to describe the transporting of ferric ion onto DSCT-adsorbent.

Keywords: ferric ion, seeds of cypress Tree, Freundlich isotherm, sorption, pseudo-second order.

1. INTRODUCTION

Heavy metals, such iron, could be found in wastewater from a number of industrial processes such as the waste from mining, refining of metals, and the combustion of fossil fuels or wood. These are considered as major sources of pollutants [1]. On the other hand, the iron ion is found in the groundwater through multiple sources such as wells located in shale, sandstone, and alluvial deposits [2]. In ground water, the level of iron ion seldom exceeds 10 mg L^{-1} [3]. Iron ion present in the form of ferric (Fe^{+3}) or ferrous (Fe^{+2}) ion, and this depends on the pH, dissolved oxygen concentration, dissolved and total organic carbon (DOC/TOC) ratio, color, humic and other organic acids, exposure to sunlight and chloride concentration [4, 5]. Ferrous ion is chemically unstable in water and exists in this state only between pH 4.0 and 5.0 in low oxygen conditions [6]. As pH and the partial pressure of oxygen (pO_2) (well-oxygenated water) increase, ferrous ion oxidizes to its ferric (Fe^{3+}) forms such as insoluble ferric hydroxide, $\text{Fe}(\text{OH})_3$. In these forms it is possible for this insoluble iron to remain suspended in solution, especially in moving waters such as rivers and streams. However, ferric ion may make a metal complex through chelating with inorganic and organic ligands and be water soluble.

Iron can be potentially toxic to the human health and causes many environmental impacts at high concentrations [3, 7-9]. Moore reviews iron as an inorganic contaminant in water and summarizes relevant production, chemistry and toxicity [10]. In case that the concentration of iron ion in the water is higher than 0.3 mg L^{-1} , it leaves macular pigment brown on the clothes while doing laundry [11]. In addition, the high concentration of iron ions in water causes foul taste and unpleasant odors. This is as a result of the emergence of bacteria that grow on the iron ion, especially in wastewater distribution mains [2]. Because of its high toxicity,

it has to be finding a variety of safe ways to reduce the high concentrations of iron ion in the water to allowable levels global.

For tracing iron ion into recommended limit, a number of chemical and physical approaches were used such as supercritical fluid extraction, bioremediation, oxidation with oxidizing agent [12-14]. Conventional methods for the removal of heavy metals from waters are often cost prohibitive. Adsorption technology is considered an alternative technology for metal sequestering to be cost-effective, efficient processes and environmentally acceptable. Recently, some studies have been directed toward using the surfaces of the natural organic or inorganic adsorbents for the removal of the iron ion from the aqueous solutions. For example, a high-level of ferric ion have been removed from a model aqueous solution using zeolite [15], activated carbon [16, 17], olive cake [18], jojoba seeds [19], quartz and bentonite [20]. Based on such recent works, natural seeds of fruits and trees can be used to remove toxic heavy metals from water. For example, cadmium ion is removed from in aqueous solution by using adsorption onto *Strychnos potatorum* seeds [21].

Cypress tree is a perennial tree, conical-shaped, about 28 meters (80 feet) high and originated from the East (Mediterranean region). It is an evergreen tree with dark green foliage, small flowers and round brown-gray cones with seed nuts inside [22]. The main components of cypress tree seeds are protein, some fatty acids (containing α -pinene, camphene, sabinene, β -pinene, d-3-carene, myrcene, α -terpinene, terpinolene, linalool, bornyl acetate, cedrol and cadinene). Oil content can be isolated through the use of cold pressing process, leaving a huge quantity of industrial residues of cypress tree seeds (called *Defatted Seeds of Cypress Tree*; DSCT). This residue could convert into raw low-cost materials and locally available adsorbents, which can be used as an adsorbent to remove ferric ion from the aquatic system. Fat

can be removed from the residues by washing cypress tree seeds in *n*-Hexan (steam distillation). This process leaves abundant proteins and cellulose. Furthermore, it increases the cellulosic pores concentrations and then increases the surface active sites in DSCT adsorbent. Generally, the DSCT adsorbent includes -OH, -COO⁻, -CN and -NH₂ functional groups. Therefore, metal ion could be adsorbed by DSCT using two suggesting sorption mechanism: i) physi-absorption of ferric ion in the cellulosic pores, and ii) chemisorptions of ferric ion in the -OH, -COO⁻, -CN and -NH₂ functional groups of the DSCT adsorbent. Wherein, this adsorbent can be considered as excellent alternatives to the chemical remediation, due to its adsorption capacity, low cost, and high availability. Studies of Defatted Seeds of Cypress Tree as an adsorbent for heavy metal are very limited. Only one recent research investigated by using the leaves of the cypress as biosorbent for removing heavy metal ions from water [23]. To the best of our knowledge, no study has been reported to remove

ferric ions from aquatic systems using DSCT. The main objective of this study is to use DSCT as a low-cost adsorbent to remove the large amount of ferric ion from water. The ferric ion is insoluble in water, but in any case is soluble in acidic aqueous solution. In addition, the sorption mechanism has not been reported yet. Therefore, it can perform multiple experiments of adsorption by changing some of the variables for each experiment. These variables could contribute to finding the optimal conditions for adsorption of ferric ion onto DSCT-adsorbent such as the contact time, and initial concentration, temperature and DSCT-adsorbent dosage. The equilibrium distribution of ferric ion between the sorbent and the solution is important in determining the maximum sorbent capacity. Isotherm models of the Langmuir and Freundlich are used to correlate experimental data of the sorption system. Kinetic models of pseudo-first-order and pseudo-second-order can test the experimental data to determine the nature of adsorption on the surface of DSCT-adsorbent.

2. EXPERIMENTAL SECTION

2.1. Material and methods.

2.1.1. Defatted Seeds of Cypress Tree (DSCT).

Defatted Seeds of Cypress Tree (DSCT) have been collected from the cypress trees that planted in Mutah University (Krak, Jordan). The seeds have been washed several times with cold distilled water where it followed that by hot distilled water. Afterwards, its oil was removed from the seeds by *n*-Hexan (steam distillation). This sample was filtered out by using filter paper (Whatman No. 41) and then dried in an oven at 50-60 °C for 24 h. The dried DSCT-adsorbent was crushed and sieved to 0.425 mm (approx.) mesh size.

2.1.2. Reagents.

All chemicals were used as received as analytical grade. Ferric ion salt of Fe(NO₃)₃·6H₂O was purchased by commercial providers from Fluka Chemika. The NaOH, HNO₃ and HCl were purchased from Merck. Stock solution (1000 mg L⁻¹) of ferric ion was prepared by dissolving exact amount of ferric salt (±0.01 g) in 1000 ml ultrapure deionised water (18 Ω cm). The standard model solutions of 30-200 mg L⁻¹ were prepared by appropriate dilution. The initial pH of the solution was adjusted using 1% HNO₃ for all experiment runs.

2.1.3. Apparatus and Instruments.

Atomic Absorption Spectrophotometer, AAS, (Model AA 100, Perkin-Elmer) was used to analyze the concentration of the ferric ion in aqueous solution. The pH of all solutions was recorded by pH meter (Orion 520). The temperature was controlled using a temperature controller (Gefellschaft Funn 1003, ±0.1 °C). Isothermal shaker was also used (Gefellschaft Fur 978). Analytical balance is used with ± 0.0001 mg (Sartorius, CP324-S/management system certified according to ISO 9001).

2.1.4. Equilibrium Studies.

The removal of ferric ion was calculated from the mass balance, which was stated as the amount of ferric ion adsorbed onto the DSCT-adsorbent. It equal the amount of ferric ion

removed from the aqueous solution. Mathematically can be expressed in Equations 1 and 2:

$$q_e = \frac{(C_i - C_e)}{S} \quad (1)$$

$$q_t = \frac{(C_i - C_t)}{S} \quad (2)$$

Where

q_e : Ferric ion amount adsorbed on the DSCT surface at equilibrium (mg g⁻¹).

q_t : Ferric ion amount adsorbed on the DSCT surface at a specific time (mg g⁻¹).

C_i : Initial concentration of ferric ion in the aqueous solution (mg L⁻¹).

C_e : Equilibrium concentration or final concentration of ferric ion in the aqueous solution (mg L⁻¹).

C_t : The final concentration of ferric ion in the aqueous solution (mg L⁻¹) at a specific time.

S : Dosage (slurry) concentration of DSCT-adsorbent and it is expressed by Equation 3:

$$S = \frac{m}{v} \quad (3)$$

where v is the initial volume of ferric ion solution used (L) and m is the mass of DSCT-adsorbent.

The percent adsorption (%) was also calculated using Equation 4:

$$\% \text{ Adsorption} = \frac{C_i - C_e}{C_i} \times 100\% \quad (4)$$

2.1.5. Effect of Dosage.

Adsorption measurements were made by a batch technique at a temperature of 50 (± 1 °C). Different doses of DSCT (2, 6, 10, 20, 30, 40 and 100 g L⁻¹) were placed in a 100 mL stopper, plastic flask containing 50 mL of aqueous ferric ion ($C_i = 100 \text{ mg L}^{-1}$, pH_i = 1.15). The solutions were shaken vigorously using thermostatic mechanical shaker for 3.0 h. The agitation speed (300 rpm) was kept constant for each run to ensure equal mixing. At the end of the equilibrium, the flasks were removed from the shaker and then the supernatant solution in each flask was filtered using filter

paper (Whatman No. 41). The filtrate samples were analyzed. All the reported results were the average of at least triplicate measurements.

2.1.6. Effect of Contact Time.

Adsorption measurements were made by a batch technique at a temperature of 50 °C (± 1 °C). The stopper, plastic flasks, containing 50 mL of initial concentrations ($C_i = 100 \text{ mg L}^{-1}$, $\text{pH}_i = 1.15$) of Ferric ion and 10 g L^{-1} of DSCT were shaken vigorously using thermostatic mechanical shaker (300 rpm) for a known period in the interval of 5 to 180 min with increment of 10 min from 10 to 60 min then 30 min from 60 to 120 min and then 60 min from 120 min to 180 min. At the end of the equilibrium, the flasks were removed from the shaker and then the supernatant solution in each flask was filtered using filter paper (Whatman No. 41). The filtrate samples were analyzed. All the reported results were the average of at least triplicate measurements.

2.1.7. Effect of Initial Concentration.

Adsorption measurements were made by a batch technique at a temperature of 50 (± 1 °C). The stopper, plastic flasks, containing 50 mL of different initial concentrations ($C_i = 30, 50, 100, 150$ and 200 mg L^{-1}) of ferric ion and 10 g L^{-1} of DSCT-adsorbent were shaken vigorously using thermostatic mechanical shaker for 3.0 h. The agitation speed (300 rpm) was kept constant for each run to ensure equal mixing. At the end of the equilibrium time, the flasks were removed from the shaker and then the supernatant solution in each flask was filtered using filter paper (Whatman No. 41). The filtrate samples were analyzed. All the reported results were the average of at least triplicate measurements.

2.1.8. Effect of Temperature.

The adsorption experiments were carried out by shaking vigorously the stopper, plastic flasks containing 50 mL of 100 mg

L^{-1} ($\text{pH}_i = 1.15$) of ferric ion and 10 g L^{-1} of DSCT-adsorbent using thermostatic mechanical shaker at constant contact time (3 h) and agitation speed (300 rpm) with varying temperatures (20, 30 and 40 °C). At the end of the equilibrium time, the flasks were removed from the shaker and then DSCT was filtered using filter paper (Whatman No. 41). The filtrate samples were analyzed. All the reported results were the average of at least triplicate measurements.

2.1.9. Isotherm and kinetic models.

The isotherm experiments were conducted by using 30, 50, 100, 150 and 200 mg L^{-1} of ferric ion solutions. The initial pH was adjusted by using 1% HNO_3 solution ($\text{pH}_i = 1.15$). The mixtures containing 0.5 g DSCT and 50 mL of ferric ion solutions were stirred under the shaking conditions of 300 rpm, 120 minutes and 50 °C. Afterwards, the flasks were removed from the shaker, and then DSCT solid was filtered by filter paper (Whatman No. 41). The filtrate supernatant solutions were analyzed. All the reported results were the average of at least triplicate measurements.

For the kinetic studies, a number of samples containing 0.5 g DSCT and 50 ml of ferric ion solutions ($C_i = 100 \text{ mg L}^{-1}$) were placed in the 100 mL flasks. The initial pH was adjusted by using 1% HNO_3 solution ($\text{pH}_i = 1.15$). These flasks were agitated using a temperature-controlled shaker ($T = 50 \text{ °C}$) at 300 rpm for 120 minutes. Afterwards, the flasks were removed from the shaker at every 10 minutes in the first 60 minutes and then 30 minutes until the end of 180 minutes. The DSCT solid was filtered using filter paper (Whatman No. 41). The filtrate supernatant solutions were analyzed. All the reported results were the average of at least triplicate measurements.

3. RESULTS SECTION

3.1. Dosage Effects.

Figure 1 clarifies the removal percentage of the ferric ion from the aqueous solutions using different dosages of DSCT-adsorbent (2, 6, 10, 20, 30, 40 and 100 g L^{-1}). Where, it shows that the removal percentage increased with increasing doses of the DSCT-adsorbent. This behavior is expected because of the increase in dose lead to increased surfaces of adsorption, and thus increases the numbers of the ferric ion that attached to adsorbent surfaces. These results in Figure 1 show that the maximum and the minimum removal of ferric ion onto DSCT-adsorbent is 76 and 73 % (approx.), respectively, according to the mentioned variables (100 g L^{-1} of DSCT-adsorbent). From another direction, we find that the increase in the dosage does not affect significantly the percentage of adsorption. This is due to the reason that the ferric ion taking the enough time (120 min.) to bind with the most functional groups in case of utilizing the low dosage of adsorbent. This means that ferric ion may create and activate of some new activation sites (functional groups) on the DSCT particles. Furthermore, this could guide us for the presence of pores inlets on the adsorbent surface. This could allow more number of ferric

ions to pass deeply inside the DSCT adsorbent. While in case of utilizing the high dosage of DSCT-adsorbent, these functional groups may not be utilized or come properly in contact with non-available enough ferric ion.

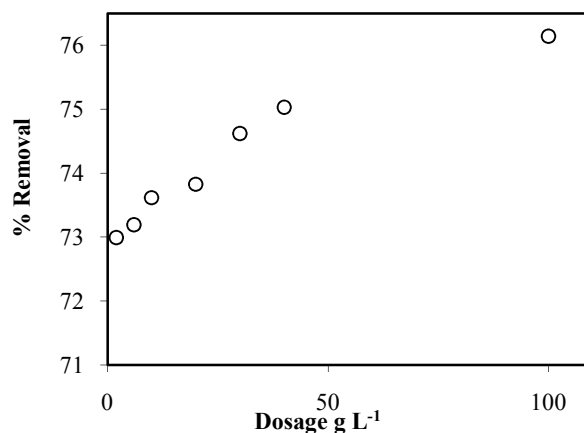


Figure 1. The effect of dosage for adsorbing ferric ion onto DSCT-adsorbent ($T = 50 \text{ °C}$, $C_i = 100 \text{ mg L}^{-1}$, 1% HNO_3 aqueous solution, rpm = 300, adsorbent dosage = 2, 6, 10, 20, 30, 40 and 100 g L^{-1} , $t = 120 \text{ min}$).

3.2. Effect of Ferric ion concentration.

The effect of ferric ion concentration on the sorption system was investigated between 30 and 200 mg L⁻¹. Figure 2 shows the percentages of removal of variant concentration of ferric ion by using 10 g L⁻¹ of DSCT- adsorbent at 50 °C and 120 minutes of contact time. It shows that the percentage of removal decreases with the increase in the initial concentration of the solutions. For example, the removal percentage was 93 % using low level concentration (30 mg L⁻¹); while it was 87 % using high-level (150 mg L⁻¹). At high-level concentrations, the available sites of adsorption become fewer. The presence of high amount of ferric ion creates a highly competitive on the pores and cracks of the adsorbent particle surfaces. This makes the surface of the adsorbent closes faster by large numbers of ferric ion, resulting in leaving many sites in the adsorbent that cannot adsorb any more of iron ion. However, we find that the increase in the initial concentration does not affect significantly the percentage of removal. This is due to the reason that the iron ion taking the enough time (120 min.) to adsorb on the surface of the 10 g L⁻¹ of DSCT-particles. This result compatible with the recent studies, for example natural olive cake [18], zeolite [15], bentonite and quartz [20] in addition to other reported example by Karthikeyan [24].

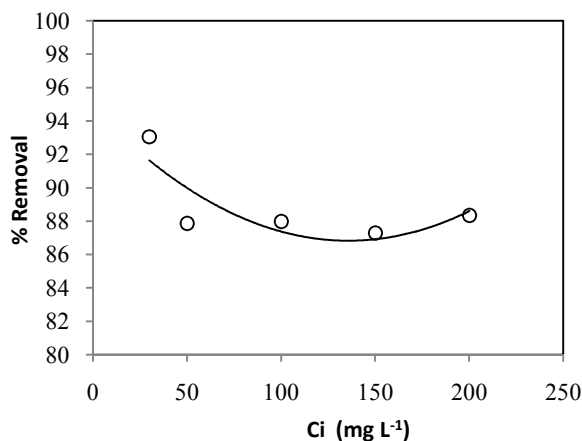


Figure 2. The effect of initial concentration for adsorbing ferric ion onto DSCT-adsorbent (T = 50 °C, C_i = 30, 50, 100, 150 and 200 mg L⁻¹, pHi = 1.15, rpm = 300, adsorbent dosage = 10 g L⁻¹, t = 120 min).

3.3. Effect of Temperature.

Figure 3 shows the percentages of removal of 100 mg L⁻¹ of ferric ion solution by using 10 g L⁻¹ of DSCT- adsorbent and 120 minutes of contact time at varying temperatures (30, 40 and 50 °C). The maximum removal percentage was 78 % (approx.) and achieved at 50 °C, while the lowest percentage was 70 % (approx.) at a temperature of 30 °C. This is due to the increase in temperature leads to accelerate the speed of ferric ion that can be transferred from a bulk solution to the adsorption sites. Thus, the ferric ion can be activated and then hasten the interaction between ferric ion and adsorbing sites [25-27]. This behaviour trend can be observed in our previous studies for the sorption of ferric ion onto various adsorbents such as using natural quartz, bentonite [20] and silica [28]. However, The chemisorptions of Fe³⁺ ions on DSCT surface has been found non-highly affected by raising the value of temperatures. This indicates to the weakly chemical interaction of ferric ion onto the DSCT surface (chemisorptions).

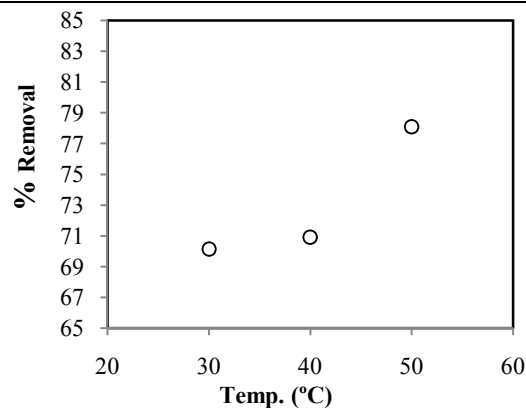


Figure 3. The effect of temperature for adsorbing ferric ion onto DSCT-adsorbent (C_i = 100 mg L⁻¹, pHi = 1.15, rpm = 300, adsorbent dosage = 10 g L⁻¹, t = 180 min).

3.4. Isotherm Modeling.

The experimental data for the adsorption equilibrium are analyzed by well-known isotherms, such as the Langmuir and Freundlich sorption models. The Langmuir sorption model is based on the theoretical principle that only a single adsorption layer (monolayer) can be formed on the outer surface of the DSCT-adsorbent and after that no further adsorption takes place. It represents the equilibrium distribution of ferric ion between the DSCT-adsorbent and aqueous phases. Therefore, this theory can be applied in this study. The linear form of the Langmuir model [29] is given by Equation 5:

$$\frac{C_e}{q_e} = \frac{1}{q_{max}b} + \frac{1}{q_{max}}C_e \quad (5)$$

A plot of C_e/q_e versus C_e , gives a straight line of slope $1/q_{max}$ and intercept $1/(q_{max}b)$ as shown in Figure 4. It can be seen that the isotherm data have yielded excellent fits within the Langmuir isotherm based on its correlation coefficient value ($R^2 = 0.991$). The value of maximum adsorption capacity, q_{max} , and adsorption affinity, b , were calculated to be 27.8 mg g⁻¹ and 0.051 L mg⁻¹, respectively. The calculated q_{max} and b in the laboratory scale has a good capacity of adsorbent and stronger adsorption affinity of ferric ion for adsorbing on DSCT. These results agree qualitatively with those published results on the use of the palm fruit bunch and maize cob for the removal of ferric ion from the aqueous phase [30].

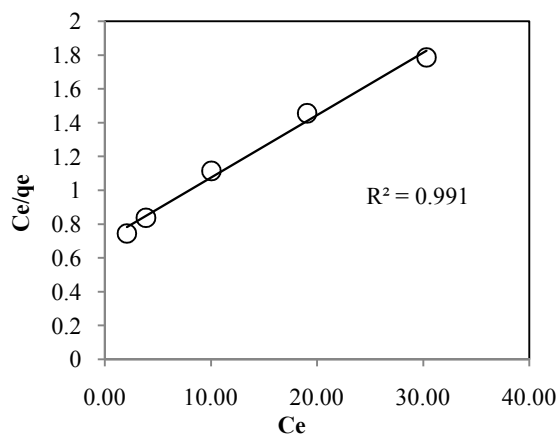


Figure 4. Linear Langmuir isotherms for adsorbing ferric ion onto DSCT-adsorbent (T = 50 °C, C_i = 100 mg L⁻¹, pHi = 1.15, rpm = 300, adsorbent dosage = 10 g L⁻¹, t = 120 min).

Freundlich model is commonly used to describe: (i) non ideal and reversible adsorption; and (ii) the adsorption

characteristics of the heterogeneous surface. The Freundlich equation does not consider all sites on the adsorbent surface to be equal. Furthermore, it is assumed that, once the surface is covered, additional adsorbed species can still be accommodated (adsorbate-adsorbate interaction). In other words, the linearized Freundlich isotherm model is expressed as in Equation 6 [31]:

$$\ln q_e = \ln K_f + \frac{1}{n} \ln C_e \quad (6)$$

The Freundlich constants K_f and n indicate the adsorption capacity and the adsorption intensity, respectively. They are calculated from the intercept and slope of the $\ln q_e$ vs. $\ln C_e$ plot (see Figure 5). It can be seen that the Freundlich model fitted the experimental data well, rather than a Langmuir isotherm model based on its correlation coefficient value ($R^2 = 0.995$). This indicates for the heterogeneous assembly of ferric ion on the DSCT surface. In this case, the Freundlich constants K_f and n were found to be 1.795 and 1.4881, respectively. The magnitudes of K_f and n show easy separation of the aqueous ferric ion and they indicate favorable adsorption. The intercept K_f value is an indication of the adsorption capacity of the adsorbent; the slope $1/n$ indicates the effect of concentration on the adsorption capacity and represents adsorption intensity or surface heterogeneity [32, 33]. It becomes more heterogeneous as its value gets closer to zero. A value below unity implies a chemisorptions process [34]. As seen, the value of “ n ” was found high enough for separation. This model has been widely applied to describe the adsorption of ferric ion onto several adsorbents such as natural bentonite (NB) [20], natural quartz (NQ) [20], olive cake (OC) [18], and chitin [24] (see Table 2).

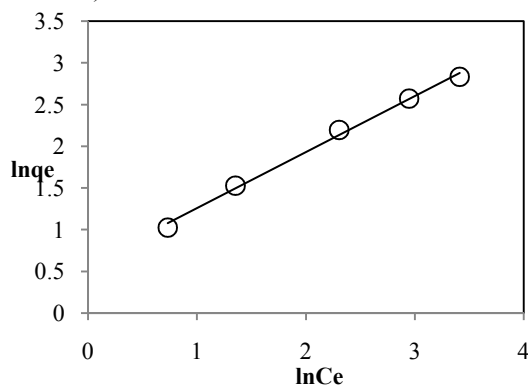


Figure 5. The linearized Freundlich isotherms for adsorbing ferric ion onto DSCT-adsorbent ($T = 50\text{ }^\circ\text{C}$, $C_i = 100\text{ mg L}^{-1}$, $\text{pHi} = 1.15$, $\text{rpm} = 300$, adsorbent dosage = 10 g L^{-1} , $t = 120\text{ min}$).

The effect of isotherm shape is discussed from the direction of predicting the weather and adsorption system is “favorable or “unfavorable”. It was previously reported [35.] that the dimensional analysis, separation factor, or equilibrium parameter “ R_L ” was as an essential feature of the Langmuir isotherm to predict adsorption system to be “favorable or “unfavorable” by Equation 7:

$$R_L = 1/(1+bC_i) \quad (7)$$

Where, C_i is the initial ferric ion concentration (100 mg L^{-1}). The calculated R_L was 0.164, indicating for the favorable adsorption.

The apparent Gibbs free energy of sorption ΔG is the fundamental criterion of spontaneity. If ΔG is negative in value, then the reaction occurs spontaneously at a given temperature. The

Gibbs free energy change ΔG can be calculated using thermodynamic Equation 8:

$$\Delta G = -RT \ln k_L \quad (8)$$

Where, R is the universal gas constant ($8.314\text{ J mol}^{-1}\text{ K}^{-1}$) and T is the absolute temperature in Kelvin and b is the equilibrium constant, related to the Langmuir constant, $b (= 0.051)$.

$$k_L = b \times M_A \quad (9)$$

where, M_A is the molar weight of ferric ion. Equilibrium constant (k_L) is equal $2848.09\text{ L mol}^{-1}$. The value of standard Gibbs free energy change (ΔG) calculated at $50\text{ }^\circ\text{C}$ is found to be $-20.038\text{ kJ mol}^{-1}$. This negative sign value shows the spontaneous nature of sorption system.

3.5. The Temkin isotherm model.

The Temkin isotherm takes into accounts of indirect interactions of the adsorbate-adsorbate (ferric ion) on adsorption isotherms. The Temkin isotherm equation assumes that the heat of adsorption is simply a function of surface coverage, and the heat of adsorption of all the molecules in layer decreases linearly with increasing uniform coverage. The Temkin isotherm proposes that the decrease in the heat of adsorption is more linear rather than logarithmic as already suggested implicitly by the Freundlich equation. The Temkin isotherm is commonly used in the form of following equation Equation 10 [36]:

$$q_e = B \ln A + B \ln C_e \quad (10)$$

where, $B = RT/b_T$, b_T is the Temkin constant related to the heat of the sorption (J mol^{-1}), A is the Temkin isotherm constant (L g^{-1}), R is the gas constant ($8.314\text{ J mol}^{-1}\text{ K}^{-1}$), and it is the absolute temperature (K).

Figure 6 shows the linear plot of Temkin isotherm of ferric ion sorption onto DSCT-adsorbent at $50\text{ }^\circ\text{C}$. The constants A and B are calculated from the intercept and slope of the plot and are listed in the Table 1. The regression parameter R^2 is calculated to be 0.973, which gave a close fit to the ferric ion adsorption onto DSCT-solid particles. Therefore, it is seen that this isotherm is applicable to the description of equilibrium data. The adsorption heat of ferric ion onto DSCT-surface was calculated ($b_T = 14.4445\text{ kJ mol}^{-1}$).

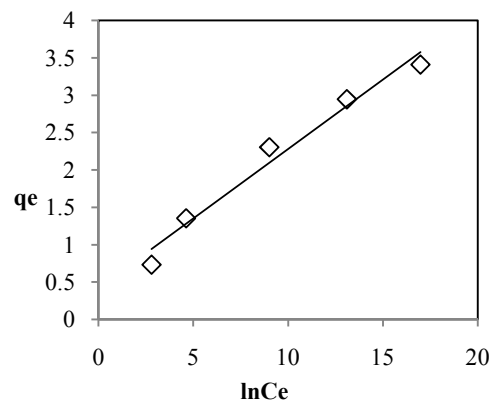


Figure 6. Temkin sorption isotherm of ferric ion onto DSCT-adsorbent ($T = 50\text{ }^\circ\text{C}$, $C_i = 100\text{ mg L}^{-1}$, $\text{pHi} = 1.15$, $\text{rpm} = 300$, adsorbent dosage = 10 g L^{-1} , $t = 120\text{ min}$).

We can note that, by comparing the values of linear regression coefficients (R^2) of the examined three isotherm models, the Freundlich model gave much better fitting Langmuir model and then Temkin model.

Table 1. The parameters for Langmuir and Freundlich.

Langmuir	T/°C	q_{max} (mg g ⁻¹)	b (L mg ⁻¹)	R^2	
	50	27.8	0.051		0.991
Freundlich	T/°C	n	k_f	R^2	
	50	1.48809	1.79499	0.995	
Temkin	T/°C	A	B	b_T	R^2
	50	9.565	0.186	14.4445 (kJ mol ⁻¹)	0.973

To justify the validity of NCS-adsorbent for the removal of ferric ion from the aqueous solution, the adsorption potentials, as shown in Table 2, have compared with the adsorbents like natural bentonite (NB) [20], natural quartz (NQ) [20], olive cake (OC) [18], natural zeolite (NZ) [15] activated carbon [16, 17], eggshell [30], chitosan [31] and chitin [32]. Apparently the maximum removal of ferric ion onto NCS-adsorbent was greater than chitin, carbon, NZ, NQ and NB adsorbents. The heterogeneity adsorption capacity for NCS-adsorbent represented by Freundlich model has matched with the heterogeneity adsorption of NB, NQ, OC and chitin adsorbents. However, the obtained results are not agreed with adsorption into carbon, chitosan, NZ and eggshell adsorbents.

Table 2. Adsorption isotherm of ferric ion onto natural adsorbents.

Adsorbents	Langmuir		Freundlich				Ref.
	q_{max} (mg g ⁻¹)	b (L mg ⁻¹)	R^2	K_f	$\frac{1}{n}$	R^2	
Natural bentonite (NB)	20.96	0.005	0.938	0.202	0.775	0.992	[20]
Natural quartz (NQ)	14.49	0.004	0.961	0.115	0.780	0.996	[20]
Olive cake (OC)	58.48	0.015	0.96	2.164	0.628	0.992	[18]
Natural zeolite (NZ)	7.35	0.014	0.998	3.353	0.106	0.954	[15]
Feldspar(NF)	25.00	0.046	0.94	1.70	0.621	0.997	[37]
Jojoba seeds (DJS)	333.33	0.0026	0.992	1.795	0.933	0.999	[19]
Natural Cotton (NCF)	49.75	0.019	0.993	1.114	0.840	0.997	[38]
Carbon	6.14	0.274	1.00				[16]
Eggshells	5.99	1.285	0.983	3.0	0.608	0.959	[43]
Chitosan	90.09	2.413	0.999	55.27	0.301	0.982	[44]
Chitin	1.40	0.2591	0.975	2.45	0.67	0.995	[25]
Coal of Date Palm Seeds (CDPS)	23.8	0.3286	0.904	2.119	2.651	0.995	[45]
DSCT	27.78	0.0511	0.991	1.795	0.672	0.995	-

3.6. Effect of Contact Time.

Adsorption of ferric ion was measured at a given contact time using a solution concentration of 100 mg L⁻¹. The plot in Figure 6 reveals that the rate of removal is higher at the beginning. This rapid adsorption of ferric ion is due to the non-reacted adsorption sites of DSCT-adsorbent, which are available in large and high at the beginning of the reaction. It is clear from Figure 7 that the removal rate increased with increasing contact time, so as to reach equilibrium after 120 min of interaction achieving the maximum removal of 77 % (approx.) (see Tables 3 and 4). In the first stage of sorption is being fast, especially during the first five min. But then the adsorption of ferric ion is being quite slow over the remaining period stages of the contact time (i.e. 5 to 120 min). This may indicate that the adsorption occurs mainly at the surface of the solid and some extent in the internal pores.

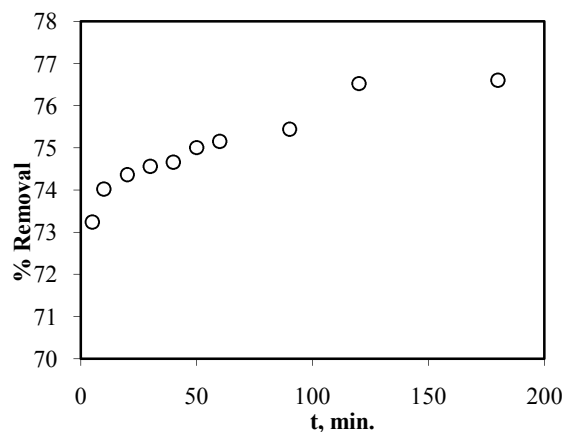

Figure 7. The effect of contact time for adsorbing ferric ion onto DSCT-adsorbent (T= 50 °C, C_i = 100 mg L⁻¹, pH_i = 1.15, rpm = 300, adsorbent dosage = 10 g L⁻¹).

Table 3. Calculated and experimental data to the pseudo-first-order model.

T (°C)	k_1 (min ⁻¹)	$q_{e, cal.}$ (mg g ⁻¹)	$q_{e, Exp.}$ (mg g ⁻¹)	R^2
50	0.085	7.66	1.11	0.666

Table 4. Calculated and experimental data to the pseudo-second-order model.

T (°C)	k_2 (g mg ⁻¹ min ⁻¹)	$q_{e, cal.}$ (mg g ⁻¹)	$q_{e, Exp.}$ (mg g ⁻¹)	R^2
50	0.197	7.66	7.69	0.999

It was found that the adsorption capacity of ferric ion onto DSCT-adsorbent, within the study conditions, is somewhat similar as using Feldspar [37], Defatted jojoba [19], and cotton fiber [38].

3.7. Kinetic Modeling.

Quantifying the changes in the sorption with time requires an appropriate kinetic model to be used. The obtained results from batch experiments have been analyzed using different kinetics models such as Lagergen pseudo first-order [39] and pseudo second-order models [40].

Lagergen pseudo first-order model is given by Equation 11:

$$\ln(q_e - q_t) = \ln q_e - k_1 t \quad (11)$$

Where q_t a ferric ion concentration is adsorbed on DSCT-adsorbent at any time (mg g⁻¹) and k_1 is the adsorption rate constant (min⁻¹). A linear plot of $\ln(q_e - q_t)$ against t gives the slope = k_1 and intercept = $\ln q_e$.

The equation that describes the pseudo-second order [40] model is given in the following linear Equation 12:

$$\frac{t}{q_t} = \frac{1}{k_2 q_e^2} t \quad (12)$$

Where, k_2 is the adsorption rate constant (g mg⁻¹ min⁻¹). Parameters of k_2 and q_e are found from the intercept and slope of t/q_t versus t linear plot, such that $q_e = 1/\text{slope}$ and $k_2 = (\text{slope})^2/\text{intercept}$. The rate constants of pseudo-first order, k_1 , and pseudo-second order, k_2 , are determined from Figures 8 and 9, respectively. These values are 0.085 min⁻¹ and 0.197 (g mg⁻¹ min⁻¹).

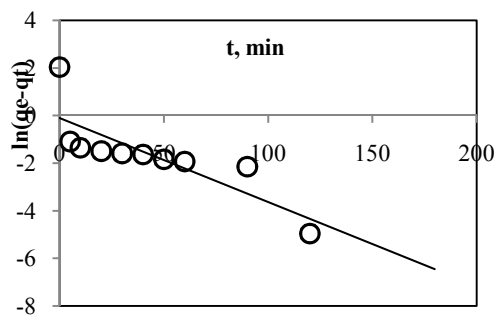


Figure 8. Legergen Pseudo-first order for adsorbing ferric ion onto DSCT-adsorbent ($T = 50\text{ }^{\circ}\text{C}$, $C_i = 100\text{ mg L}^{-1}$, $\text{pHi} = 1.15$, $\text{rpm} = 300$, adsorbent dosage = 10 g L^{-1}).

The goodness degree of the linear plot can be judged from the value of the determination coefficient (R^2). Figures 8 and 9 show that R^2 is equal 0.666 and 0.999, respectively. The adsorption of ferric ion on the DSCT-adsorbent is regarded as pseudo second-order rather than pseudo-first-order estimating a chemisorptions process. According to adsorption rate constants as shown in Tables 3 and 4, ferric ion is faster adsorbed on the DSCT-adsorbent for pseudo second-order kinetics model. This was confirmed by the equilibrium contact time that determined from their kinetic curves.

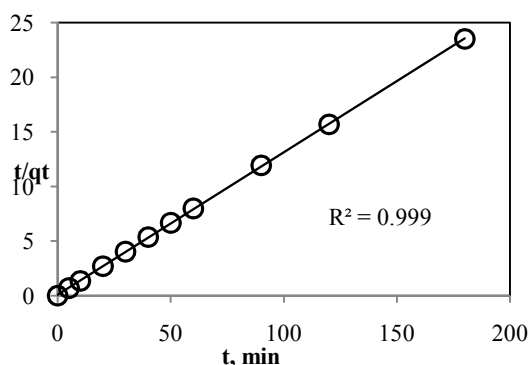


Figure 9. Pseudo-second order for adsorbing ferric ion onto DSCT-adsorbent ($T = 50\text{ }^{\circ}\text{C}$, $C_i = 100\text{ mg L}^{-1}$, $\text{pHi} = 1.15$, $\text{rpm} = 300$, adsorbent dosage = 10 g L^{-1}).

Table 5. Adsorption kinetics of ferric ion onto various natural adsorbents.

Adsorbents	Pseudo-first order		Pseudo-second order			Ref
	k_1 (min^{-1})	R^2	k_2 ($\text{g mg}^{-1}\text{ min}^{-1}$)	q_e	R^2	
Natural bentonite (NB)	0.066	0.89	0.337	0.649	0.99	[20]
Natural quartz (NQ)	0.057	0.76	0.552	0.746	0.99	[20]
Olive cake (OC)	0.061	0.89	0.018	15.97	0.99	[18]
Natural zeolite (NZ)	0.045	0.88	0.040	20.00	1.0	[15]
Feldspar(NF)	0.378	0.83	0.035	8.85	1.0	[37]
Jojoba seeds (DJS)	0.053	0.77	0.181	6.45	1.0	[19]
Cotton Fibers (NCF)	0.035	0.826	0.657	8.93	1.0	[38]
Carbon			0.048	13.04	1.0	[16,45]
Eggshells			0.403	1.92	1.0	[43]
Chitosan	0.0306	0.96	0.032		1.0	[44]
Coal of Date Palm Seeds (CDPS)	0.011	0.592	0.10242	3.534	0.99	[45]
DSCT	0.085	0.666	0.197	7.69	1.0	-

The pseudo-first-order and pseudo-second order kinetic models could not identify the diffusion mechanism. Thus to determine the diffusibility of the ferric ion into the pores of the DSCT-adsorbent, Weber-Moris intraparticle diffusion model [41] can be used in the form Equation 13:

$$q_t = k_{\text{int}} t^{0.5} + C \quad (13)$$

Where C is constant, q_t the amount of ferric ion adsorbed at a time (mg g^{-1}) and k_{int} is the intra-particle diffusion rate constant ($\text{mg g}^{-1}\text{ min}^{-0.5}$). A plot of q_t vs. $t^{0.5}$ giving straight line confirms an intra-particle diffusion sorption as shown in Figure 10. The plot is not totally linear and the moreso do not pass through the origin. This is indicative of some degree of boundary layer control and this further show that the intra-particle diffusion could not be the only mechanism involved. This plot presents multi-linearity, which it indicates that two or more steps occur. The first, sharper portion (ca. $t^{0.5}$ range from 0 to $0.87\text{ min}^{0.5}$; i.e. from 0 up to 5 min of adsorption period) is the external surface adsorption or instantaneous adsorption stage. It is non-controlled and fast adsorption process. The second portion is the gradual adsorption stage (ca. $t^{0.5}$ range from 0.87 to $0.982\text{ min}^{0.5}$; i.e. from 5 up to 40 min of adsorption period), where the intraparticle diffusion is rate-controlled. The third portion is the final equilibrium state where the intraparticle diffusion starts to slow down due to extremely low solute concentrations in the solution and chemisorptions stage is taken part on the DSCT surface and pores (which already has been successfully explained by pseudo-second order kinetic model from 40 to 180 min of adsorption period).

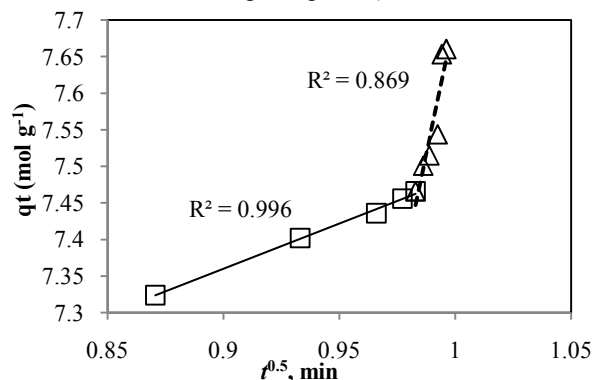


Figure 10. Weber-Moris intra-particle diffusion kinetic model for adsorption of ferric ion on DSCT-adsorbent starting ($T = 50\text{ }^{\circ}\text{C}$, $C_i = 100\text{ mg L}^{-1}$, $\text{pHi} = 1.15$, $\text{rpm} = 300$, adsorbent dosage = 10 g L^{-1} , $t = 0\text{-}180\text{ min}$).

Film diffusion mass transfer rate equation is presented by Equation 14:

$$\ln\left\{1 - \frac{qt}{qe}\right\} = -k t \quad (14)$$

Where, k (min^{-1}) is the liquid film diffusion constant. A plot of $\ln[1 - (q_t/q_e)]$ vs. t should be a straight line with a slope $-k$ if the film diffusion is the rate limiting step [42]. Figure 11 shows the film diffusion mass transfer stage from 5 to 90 min of adsorption process. Therefore, this stage could be considered as the rate controlling and limiting step with the value of $k = 0.011\text{ min}^{-1}$.

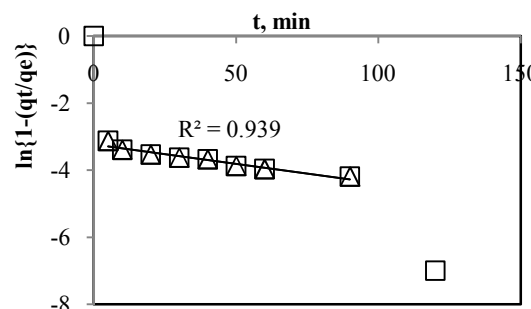


Figure 11. Film diffusion mass transfer rate model presented by Boyd et al [38] ($T = 50\text{ }^{\circ}\text{C}$, $C_i = 100\text{ mg L}^{-1}$, $\text{pHi} = 1.15$, $\text{rpm} = 300$, adsorbent dosage = 10 g L^{-1} , $t = 0\text{-}180\text{ min}$).

4. CONCLUSIONS

Defatted Seeds of Cypress Tree (DSCT-adsorbent) has the ability to remove ferric ion from aqueous systems. Where we can achieve the highest removal for the aqueous ferric ion (ca. 94 %) by applying the following parameters: low initial concentration of ferric ion (30 mg L⁻¹), 100 g L⁻¹ dosage of the DSCT-adsorbent, 50 °C, 120 min of contact time, and 300 rpm. Freundlich isotherm is applicable to describe the equilibrium data. Sorption of the ferric ion into DSCT surface is heterogeneous, favorable and spontaneous in nature. Sorption process is associated with uncontrolled rate during the first 5 min of contact time achieving the removal percentage of 76 %. The mechanism of adsorption is detected as chemisorptions, which explained by pseudo-second

order kinetic model, especially from 40 to 180 min of adsorption period. The chemisorptions of ferric ion onto DSCT-adsorbent is the rate limiting step ($R^2 = 0.999$). We can describe the adsorption mechanism of ferric ion on DSCT through three steps: (i) the uncontrolled rate of the external surface adsorption or instantaneous adsorption stage within 0 to 5 min of adsorption period. (ii) The intraparticle diffusion stage within 5 up to 40 min of adsorption period. (iii) Chemisorptions stage and final equilibrium stage within 40 to 180 min of adsorption period. This approach can be applied and recommended for purifying drinking water resources by using the DSCT material as natural membrane.

5. REFERENCES

- [1] Sterner O., Chemistry, *Health and Environment*, 2ed Ed., 355-363, **2010**.
- [2] Viessman W., Hammer M.J., Perez E.M., Chadik P.A., *Water Supply and Pollution Control*, 8th Ed., 438-440, **2009**.
- [3] Manahan S.E., *Environmental Chemistry*, 8th Ed., 211-213, **2010**.
- [4] Davison W., DeVitre R., Iron particles in the fresh water, *Environmental particles*, Vol. 1, *Environmental analytical and physical chemistry series*, 1st Ed., **1982**.
- [5] Stumm W., Morgan J.J., *Aquatic Chemistry*, 2ed Ed. Wiley, New York, NY, USA, **1981**.
- [6] Freda J., The effects of aluminum and other metals on amphibians, *Environmental Pollution*, 71, 305-328, **1991**.
- [7] Sarin P., Snoeyink V.L., Bebee J., Jim K.K., Beckett M.A., Kriven W.M., Clement J.A., Iron release from corroded iron pipes in drinking water distribution systems: Effect of dissolved oxygen, *Water Research*, 38, 1259-1269, **2004**.
- [8] Das B., Hazarika P., Saikia G., Kalita H., Goswami D.C., Das H.B., Dube S.N., Dutta R.K., Removal of iron from groundwater by ash: A systematic study of a traditional method, *Journal of Hazardous Materials*, 141, 834-841, **2007**.
- [9] Walker C.H., Sibly R.M., Hopkin S.P., Peakall D.B., *Principle of Ecotoxicology*, 4th Ed. CRC press, Taylor and Francis Group, USA, 3-7, **2012**.
- [10] Moore J.W., Iron in: Inorganic contaminants of surface water, Research and Monitoring Priorities, *Springer series on environmental management*, 13, 140-154, **1991**.
- [11] Drinan J.E., Water and Wastewater treatment: A Guide for the Non-Engineering Professional, CRC press LLC, *Technomic Publishing USA*, 30-41, **2001**.
- [12] Andersen W.C., Bruno T.J., Application of gas-liquid entraining rotor to supercritical fluid extraction: removal of iron (III) from water, *Analytica Chimica Acta*, 485, 1-8, **2003**.
- [13] Ellis D., Bouchard C., Lantagne G., Removal of iron and manganese from groundwater by oxidation and microfiltration, *Desalination*, 130, 255-264, **2000**.
- [14] Katircioglu H., Aslm B., Rehber Turker B., Atic T. Beyatl Y., Removal of cadmium(II) ion from aqueous system by dry biomass, immobilized live and heat-inactivated *Oscillatoria* sp. H1 isolated from freshwater (Mogan Lake), *Bioresource Technology*, 99, 4185-4191, **2008**.
- [15] Al-Anber M., Al-Anber Z., Utilization of natural zeolite as ion-exchange and sorbent material in the removal of iron, *Desalination*, 225, 70-81, **2008**.
- [16] Edwin Vasu A., Adsorption of Ni(II), Cu(II) and Fe(III) from aqueous solution using activated carbon, *E-Journal of Chemistry*, 5, 1-9, **2008**.
- [17] Kannan N., Veemaraj T., Removal of Lead(II) Ions by Adsorption onto Bamboo Dust and Commercial Activated Carbons-A Comparative Study, *E-Journal of Chemistry*, 6, 2, 247-256, **2009**.
- [18] Al-Anber Z., Al-Anber M., Adsorption of ferric ion from aqueous solution by olive cake: Thermodynamic and kinetic studies, *Journal of the Mexican Chemical Society*, 52, 108-115, **2008**.
- [19] Al-Anber M.A., Al-Anber Z.A., Al-Momani I., Al-Momani F., Abu-Salem Q., The performance of defatted Jojoba seeds for the removal of toxic high-concentration of the aqueous ferric ion, *Desalination and Water Treatment*, 52, 1-3, 293-304, **2014**.
- [20] Al-Anber M., Removal of High-level Fe³⁺ ion from aqueous solution using Jordanian inorganic materials: Bentonite and Quartz, *Desalination*, 250, 885-891, **2010**.
- [21] Saif M.M.S., Siva Kumar N., Prasad M.N.V., Binding of cadmium to *Strychnos potatorum* seed proteins in aqueous solution: Adsorption kinetics and relevance to water purification, *Colloids and Surfaces B: Biointerfaces*, 94, 73-79, **2012**.
- [22] <http://www.essentialoils.co.za/essential-oils/cypress.htm>
- [23] Wan Ngah W.S., Hanafiah M., Removal of heavy metal ions from wastewater by chemically modified plant wastes as adsorbents: a review, *Bioresource Technology*, 99, 3935-3948, **2008**.
- [24] Karthikeyan G., Andal N.M., Anbalagan K., Adsorption studies of Fe(III) on chitin, *Journal of Chemical Sciences*, 117, 6, 663-672, **2005**.
- [25] Babel S., Kurniawan T.A., Low-cost adsorbents for heavy metals uptake from contaminated water: a review, *Journal of Hazardous Materials*, 127, 1-13, **2005**.
- [26] Loizidou M.D., Grigoropoulou H.P., Ion exchange studies on natural and modified zeolites and the concept of exchange site accessibility, *Journal of Colloid and Interface Science*, 275, 570-576, **2004**.
- [27] Johnson B.B., Effect of pH, temperature and concentration on the adsorption of cadmium on goethite, *Environmental Science and Technology*, 24, 112-118, **1990**.
- [28] El-Hasan T., Al-Anber Z., Al-Anber M., Batarseh M., Al-Nasr F., Ziadat A., Kato Y., Jiries A., Removal of Zn²⁺, Cu²⁺ and Ni²⁺ ions from aqueous solution via Tripoli: simple component with single phase model, *Current World Environment*, 3, 1-14, **2008**.
- [29] Langmuir I., The constitution and fundamental properties of solids and liquids, *Journal of the American Chemical Society*, 38, 2221-2295, **1916**.
- [30] Nassar M.M., Ewida K.T., Ebrahiem E.E., Magdy Y.H., Mheadi M.H., Adsorption of iron and manganese ions using low-cost materials as adsorbents, *Adsorption Science and Technology*, 22, 25-37, **2004**.
- [31] Butt H.J., Graf K., Kappl M., *Physics and Chemistry of Interfaces*, 185-193, **2003**.
- [32] Kinniburgh D.G., Isotherm: A computer program for analyzing adsorption data, Report WD/ST/85/02. Version 2.2, *British Geological Survey*, Wallingford. England, **1985**.
- [33] Kinniburgh D.G., General purpose adsorption isotherms, *Environmental Science and Technology*, 20, 895-904, **1986**.
- [34] Foo K.Y., Hameed B.H., Insight into the modeling of adsorption isotherm systems, *Chemical Engineering Journal*, 156, 2-10, **2010**.
- [35] Al-Anber M., Thermodynamics Approach in the Adsorption of Heavy Metals, J.C. Moreno-Pirajan, *Thermodynamics-Interaction Studies-Solids, Liquids and Gases Book*: 1st Edition, In-Tech, 27, 737-764, **2011**.
- [36] Temkin M.J., Pyzhev V., Kinetics of ammonia synthesis on promoted iron catalysts, *Acta physicochimica U.R.S.S.*, 12, 217-222, **1940**.
- [37] Al-Anber M., Adsorption modeling and decontamination of aqueous Fe⁺³ ions using Jordanian Feldspar (JF), *International Journal of Environmental Science and Technology*, 12, 139-150, **2015**.

- [38] Al-Anber M., Adsorption properties of aqueous ferric ion on the natural cotton fiber: Kinetic and thermodynamic Studies, *Desalination and Water Treatment*, 52, 13-15, 2560–2571, **2014**.
- [39] Lagergren S., Zurtheorie der sogenannten adsorption gelösterstoffe, Kungliga, Svenska Vetenskapsakademiens, *Handlingar*, 24, 1-39, **1898**.
- [40] Ho Y.S., McKay G., Pseudo-second order model for sorption processes, *Process Biochemistry*, 34, 451–465, **1999**.
- [41] Weber Jr., Digiano F.O., Process dynamics in environmental system, *Environmental Science and Technology Series*, 89-94, **1996**.
- [42] Boyd G.E., Adamson A.W., Myers L.S., The exchange adsorption of ions from aqueous solutions by organic zeolites. II. Kinetics, *Journal of the American Chemical Society*, 69, 11, 2836-2848, **1947**.

- [43] Yeddou N., Bensmaili A., Equilibrium and kinetic of iron adsorption by eggshells in a batch system: Effect of temperature, *Desalination*, 206, 127–134, **2007**.
- [44] Wan Ngah W.S., Ab Ghani S., Kamari A., Adsorption Behaviour of Fe(II) and Fe(III) ions in aqueous solution on chitosan and cross-Linked chitosan beads, *Bioresource Technology*, 96, 443-450, **2005**.
- [45] Al-Anber M., Abu-Rayyan A., Almogbel M., Removal of Inorganic Ferric Ion from Water by using Coal of Date Palm Seeds (CDPS), *Biointerface Research in Applied Chemistry*, **2016**. (Accepted)

6. ACKNOWLEDGEMENTS

M. Al-Anber would like to thank Mutah University (Jordan) for giving him an annual leave (without pay) during the years 2012-2016.

© 2016 by the authors. This article is an open access article distributed under the terms and conditions of the Creative Commons Attribution license (<http://creativecommons.org/licenses/by/4.0/>).